American Mineralogist, Volume 77, pages 592–604, 1992

Ternary feldspar crystallization in high-temperature felsic magmas

HANNA NEKVASIL
Department of Earth and Space Sciences, State University of New York, Stony Brook, New York 11794-2100, U.S.A.

ABSTRACT

Ternary feldspars crystallizing at equilibrium under conditions of high temperature and low H_2O content in trachytic and dry granitic magmas show distinctly different evolutionary paths once two feldspars are stabilized if crystallization occurs under conditions of fixed H_2O activity (H_2O buffered) or under conditions in which the H_2O content increases in the melt as a result of precipitation of anhydrous minerals (H_2O unbuffered). The latter condition leads to feldspar paths characterized predominantly by decreasing Or content in plagioclase (with only slight changes in An content) and significant increases in Or content in alkali feldspar with decreasing temperature. Unlike the case for H_2O-buffered conditions, H_2O-unbuffered conditions can result in a path that includes a stage of partial resorption of plagioclase by reaction with melt, producing alkali feldspar, followed by a stage of coprecipitation of both feldspars as the H_2O content builds up and the odd (peritecticlike) region of the 2 feldspar + L or 2 feldspar + Qz + L surface shifts farther toward albite. The effect of increasing bulk H_2O or Qz content is to decrease the extent of Or enrichment in alkali feldspar, the amount of Or depletion in plagioclase, and the amount of resorption of plagioclase. The effect of decompression is complex and depends on the stage of evolution of the magma when decompression commences. Decompression can lead to crystallization or resorption of either feldspar, as well as significant changes in the compositions of the feldspars.

INTRODUCTION

Compositionally, quartz-normative trachytes and syenites differ only slightly from rhyolites and granites in having higher normative feldspar and lower quartz contents. Yet the presence of ternary feldspar and anhydrous ferromagnesian minerals indicate high temperatures and potentially significantly different crystallization pathways. The differences in crystallization pathways of the feldspars are controlled by the changes in topology of the equilibrium phase relations with decreasing H_2O content or H_2O activity in the melt. The most significant topologic change in the synthetic granite system, i.e., the system $NaAlSi_3O_8$-$CaAl_2Si_2O_8$-$KAlSi_3O_8$-SiO_2-H_2O, is the termination of the 2 feldspar + L curve, which occurs inside the feldspar subsystem instead of at the Ab-Or boundary, and the termination of the 2 feldspar + Qz + L curve, which occurs within the An-bearing granite system instead of in the haplogranite system, i.e., the system Ab-Or-Qz at low H_2O contents. This topologic change results in peritecticlike (or odd) behavior in which the reaction between a feldspar and melt produces a second feldspar at the expense of the reacting feldspar at some point along each of these curves. As recognized by Carmichael (1963) and Nekvasil (1990), the most common reaction would be the production of alkali feldspar through the reaction of plagioclase with melt. Such behavior can readily explain the presence of partially resorbed cores of ternary plagioclase (generally andesine oligoclase) within ternary alkali feldspar (generally anorthoclase sodic sanidine) reported in numerous trachytes and syenites, e.g., Sierra el Virulento (Moll, 1981), Kane Springs Wash caldera, Nevada (Novak and Mahood, 1986), Turritable Falls, southeast Queensland (Ewart, 1981).

Details of the positional relations between the solvus and the 2 feldspar + L curve (and the 2 feldspar + Qz + L curve) at low H_2O contents were calculated by Nekvasil (1990) and Nekvasil and Lindsley (1990). These calculations permitted the determination of the compositional regions in which magmas must lie if partial or complete resorption of plagioclase were to occur during equilibrium crystallization. This resorption is a consequence of the high proportion of alkali feldspar in the trachytic compositions and the more An-rich nature of this feldspar relative to the melt, which requires resorption of some plagioclase to release An for further crystallization of alkali feldspar. Nekvasil (1990), however, calculated crystallization paths only for the case in which the activity of H_2O remained unchanged during equilibrium crystallization (H_2O-buffered crystallization). In this case, the relative positions of the solvus and the 2 feldspar + L curve remain fixed during crystallization, and the resulting resorptional behavior and feldspar compositional variations can be readily shown in a ternary section of the feldspar-H_2O system.

From the discussions of Tuttle and Bowen (1958), Carmichael (1963), Abbott (1978), and Nekvasil (1990), it can be concluded that feldspar crystallization in high-

0003–004X/92/0506–0592$02.00

temperature trachytic magmas will involve at least partial resorption of plagioclase if the H_2O activity of the melt is buffered. Although there are some natural processes that could buffer the H_2O activity of the magma, such as the crystallization of a hydrous mineral or perhaps the presence of a large quantity of a mixed volatile fluid, there is no reason to expect that syenites will crystallize under buffered conditions. In granitic rocks there is abundant petrographic and textural evidence indicating an increase in H_2O activity during crystallization. Crystallization under H_2O-unbuffered conditions is probably also the more relevant process for trachytic magmas.

During normal H_2O-unbuffered crystallization of anhydrous minerals, the H_2O content of the magma increases, and the relative positions of the ternary feldspar solvus and the relevant H_2O-isoactivity three-phase (Pl + Af + L) curve in the feldspar system or the four-phase (Pl + Af + Qz + L) curve in the granite system change continually as the temperature is depressed. Additionally, as shown schematically in Figure 1, the three- and four-phase H_2O-isoactivity curves continually lengthen, and the location of the neutral point on each of these curves (where the curve begins to exhibit peritecticlike behavior) lies progressively at a higher Ab content at higher activity of H_2O (see Nekvasil, 1990, for further discussion). Importantly, however, although evolution along the 2 feldspar + L or 2 feldspar + L + Qz surfaces on the Ab side of the neutral curve is a necessary condition for resorptional behavior, it is not a sufficient condition, as shown by Nekvasil (1990). The bulk composition dictates whether or not resorption will take place during equilibrium crystallization in the odd region of each surface. Should the bulk composition permit resorptional behavior, the melt composition at which resorptional behavior is first manifested is not necessarily at the neutral curve and is also dependent upon the bulk composition. As discussed by Nekvasil (1990), the higher the bulk An content, the farther the melt must evolve along the surface past the neutral curve before resorptional behavior is manifested.

Whether or not resorptional behavior will be manifested during H_2O-unbuffered equilibrium crystallization is dependent on the relative rates of increase of H_2O content in the melt during crystallization of anhydrous phases and on the Ab enrichment of the melt during crystallization of two feldspars. The increase in H_2O content of the melt during crystallization of anhydrous phases continually shrinks the resorptional field by shifting the neutral point toward Ab and quite likely away from the melt composition. The Ab enrichment of the melt during crystallization of two feldspars, in contrast, drives the melt deeper into the resorptional field with decreasing temperature. These two competing factors lead to several questions. Would the H_2O content of unbuffered trachytic magmas increase so quickly during equilibrium crystallization as to inhibit partial resorption of plagioclase, or might partial resorption occur during the early stages of crystallization and be followed by reprecipitation of both

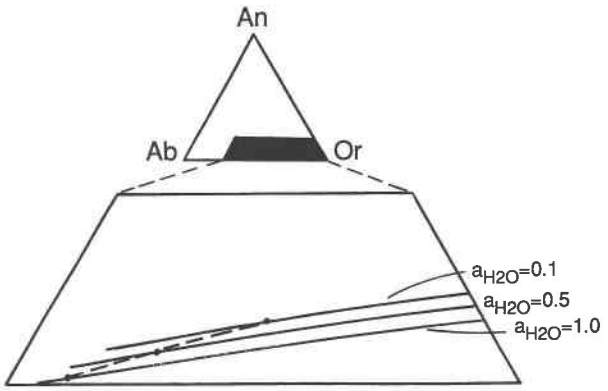

Fig. 1. Schematic diagram of the 2 feldspar + L surface in the system Ab-Or-An-H_2O shown by three H_2O-isoactivity curves. The effect of decreasing H_2O content is to shorten each curve, resulting in termination of the surface farther and farther within the feldspar system (in projection) and away from the Ab-Or sideline. The neutral point on each H_2O-isoactivity 2 feldspar + L curve, which bounds the region of even (or cotecticlike) behavior and odd (or peritecticlike) character of each curve, also shifts farther from the termination with decreasing H_2O content. The dashed curve, which connects the neutral points, divides the even portion of the surface (to the right of the curve) and the odd portion of the surface.

feldspars as a cotectic region of the 2 feldspar + L (or 2 feldspar + Qz + L) surface is reached? What effect might such a path have on the evolution of the feldspar compositions? Is the evolutionary path of the feldspar compositions significantly different from the buffered case to permit any preserved feldspar zoning in trachytes and syenites to be used to indicate the behavior of H_2O in the natural magma? What is the effect of the continually increasing Qz concentration of the melt? Is the evolution of a trachytic magma distinguishable from that of a granitic magma during the late stages?

In order to answer these questions, the controls on feldspar composition must be understood. The compositional path taken by any feldspar during crystallization is a combination of two limiting path vectors. One vector involves a decrease in An content and an increase in Or content of plagioclase. For alkali feldspar it involves a decrease in Or and increase (or slight decrease) in An in alkali feldspar. These paths are very similar to those followed by feldspars crystallizing along an almost isothermal solvus. This compositional vector is the result of the increasing Ab content of the melt and hence of the bulk feldspar compositions with continued crystallization. The other vector involves a decrease in Or content of plagioclase and an increase in Or content of the alkali feldspar with decreasing temperature as the isothermal solvus sections widen because of increasing nonideality of the solid solutions with decreasing temperature. This can be seen in Figure 2 by tie lines connecting equilibrium feldspar compositions on the ternary feldspar solvus of Lindsley and Nekvasil (1989) for a constant bulk feldspar com-

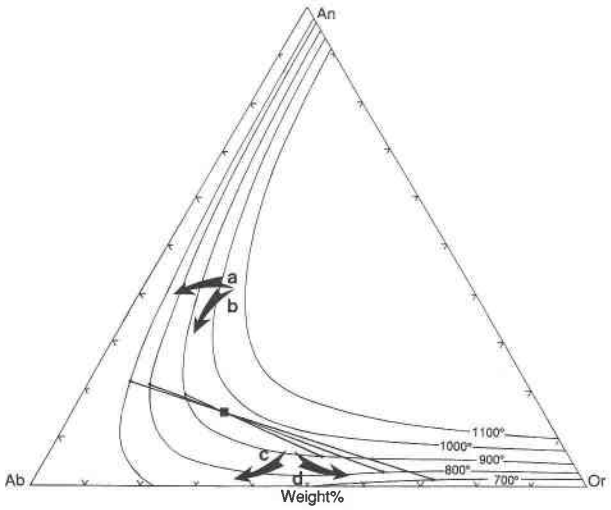

Fig. 2. The ternary feldspar solvus, calculated using the model of Lindsley and Nekvasil (1989), as a series of isothermal solvus sections (temperature in degrees Celsius). Three tie lines are shown for the same bulk feldspar composition (solid circle) at 900, 800, and 700 °C. They indicate that the equilibrium plagioclase compositions become more Or poor and the coexisting alkali feldspars more Or rich at lower temperatures. The arrows indicate the possible compositional evolutionary paths of feldspars during crystallization. If the effect of temperature on widening the solvus is dominant over the effect of the increase in Ab content of the bulk feldspar composition (because of the increase in Ab content of the melt during crystallization), plagioclase compositions may evolve along a path such as that labeled a, while alkali feldspar evolves along a path such as that labeled d. In contrast, if the changing melt composition is dominant, path b may be followed by plagioclase and path c by alkali feldspar.

position. If the dominant effect on feldspar compositions is the increase in Ab content of the melt and change in bulk feldspar composition toward Ab, then plagioclase compositions will follow a path with the characteristics of arrow b in Figure 2, and alkali feldspar a path with the characteristics of arrow c. Because of the shallower T-X slope around the nose of the solvus, however, it may be possible that for high temperature magmas, expansion of the solvus with decreasing temperature is dominant over the changing melt composition, and paths such as path a for plagioclase and path d for alkali feldspar might be followed. In this case, should feldspar crystallize in a stepwise fractional crystallization process, plagioclase will become normally zoned with respect to Or content instead of An content, while alkali feldspar develops reverse zoning in Or content.

In order to evaluate the relative magnitude of each compositional vector and to answer the questions posed above, crystallization paths were calculated using a modification of the method of Nekvasil (1988a), the ternary feldspar solution model of Lindsley and Nekvasil (1989), and the melt solution model of Nekvasil (1986) and Burnham and Nekvasil (1986). A modification to the

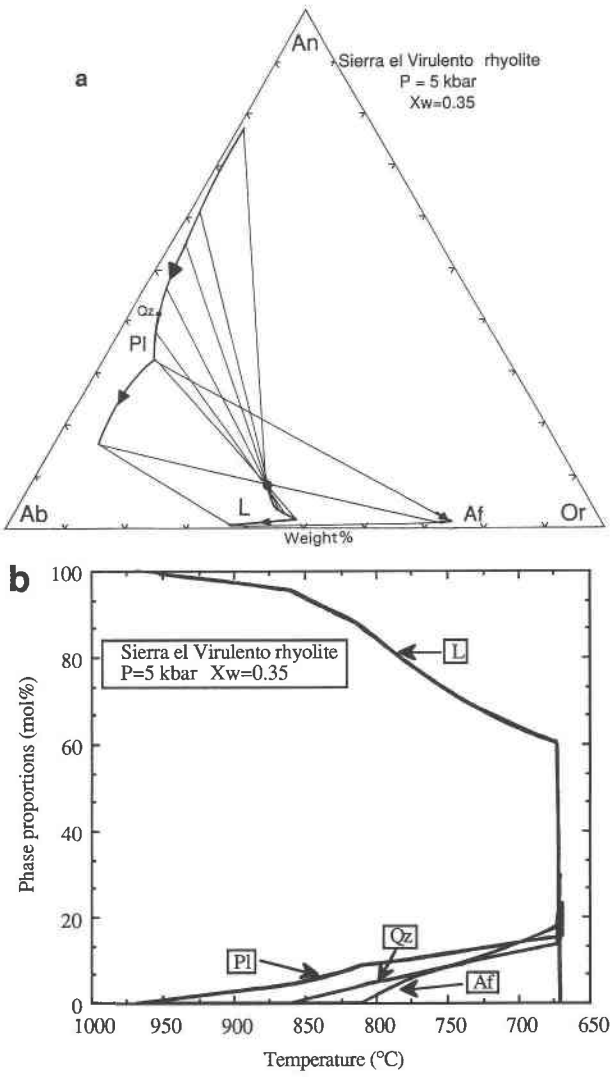

Fig. 3. Calculated H_2O-unbuffered equilibrium crystallization path for a model Sierra el Virulento rhyolite (trachyte + Qz) (28.5 wt% Or, 37.7 wt% Ab, 6.27 wt% An, 27.6 wt% Qz) at 5 kbar and 3.5 wt% bulk H_2O content. (**a**) Melt (L), plagioclase (Pl), and alkali feldspar (Af) compositions projected into the feldspar system. The symbol Qz indicates the onset of crystallization of quartz. Arrowheads point to the direction of decreasing temperature. (**b**) Variations in proportions (mol%) of melt (L), plagioclase (Pl), alkali feldspar (Af), and quartz (Qz) vs. temperature during equilibrium crystallization. The phase proportions sum to $(1 - X_{H_2O}) \times 100$.

method of Nekvasil (1988a) was required because iteration convergence is very sensitive to the chosen starting compositions in the albitic region of the ternary feldspar system. A less efficient, but more readily convergent, method for the calculation of crystallization paths was used that involved the location of the three- or four-phase isoactivity curve for a given H_2O content of the melt and bulk H_2O content, and hence a given fraction of liquid. Then the composition was shifted along the curve until the solution of the mass balance equations yielded the

chosen fraction of liquid. As concluded by Nekvasil and Lindsley (1990), the use of several other available solid solution models does affect the location and temperature of the three- and four-phase curves for a given H_2O activity; however, the crystallization trends are unaffected.

For modeling purposes a trachytic composition from Sierra el Virulento was used. This composition falls within the range of bulk compositions of trachytes and syenites in which phenocrysts of ternary anorthoclase sodic sanidine have been reported to contain irregular cores of andesine oligoclase (see Nekvasil, 1990, for more details). The trends reported here are general and should hold for most syenites and trachytes, although the specific feldspar and melt compositions attained at any stage of differentiation will differ for each bulk composition.

Feldspar crystallization in H_2O-rich granitic magmas

Feldspar crystallization trends of quartz-normative trachytic magmas should contain elements of the crystallization trends of both Qz-saturated granitic magmas and compositions in the pure feldspar system. Much experimental effort has been expended in the determination of the feldspar crystallization trends of granitic magmas (e.g., Tuttle and Bowen, 1958; Johannes, 1978). Although the determination of precise trends is problematic because of kinetic difficulties (Johannes, 1978), the available experimental data and complementary computational results involving use of thermodynamic solution models and mass balance constraints (Nekvasil, 1988a, 1988b) support the common opinion that feldspar crystallization in H_2O-unbuffered granitic magmas follows general trends similar to those in the binary feldspar systems, i.e., Ab enrichment with decreasing temperature.

Figure 3 shows the calculated H_2O-unbuffered path, in which the H_2O content of the melt is free to change upon the crystallization of anhydrous phases, of a bulk composition that was obtained by artificially increasing the silica content of a Sierra el Virulento trachyte composition (Moll, 1981) through projection toward Qz until the composition lies in the main compositional field of standard granites, according to Tuttle and Bowen (1958). For this composition at 5 kbar and 3.5 wt% bulk H_2O content ($X_{H_2O} = 0.35$, where X_{H_2O} is the mole fraction of H_2O in the system), plagioclase is the liquidus phase but is joined by quartz before alkali feldspar becomes stable. Until the magma becomes saturated in alkali feldspar, the plagioclase compositions describe a smooth curve with decreasing An and slightly increasing Or contents. Eventually, the solvus is intersected, and two feldspars are stabilized. Upon further crystallization, both feldspars change composition along a set of curves across the solvus dome that, if joined, describe a polythermal solvus section. The polythermal solvus section described by the feldspar compositions involves changes in both temperature and bulk feldspar composition as crystallization proceeds. The path of compositional evolution of the feldspars described by such a section differs from an isothermal solvus section because the path crosses innumerable isothermal sections that are progressively widening as the temperature drops. Importantly, the section of the solvus traversed by the feldspars in wet, low-temperature granitic magmas is not very sensitive to temperature. This is illustrated in Figure 3a, where the path of feldspar compositional change still retains the general shape of an isothermal section but shows little change in Or content over the considerable temperature range of crystallization under H_2O-unbuffered conditions. For this H_2O-rich composition, the plagioclase compositions will evolve predominantly by a decrease in An content. Alkali feldspar compositions, in contrast, will exhibit little change in composition. They do, however, indicate an important feature. While the magma is still H_2O undersaturated, the widening of the solvus with decreasing temperature is the dominant effect, driving the alkali feldspar composition toward Or (cf. Fig. 2). Once H_2O saturation has been attained, however, the changes in temperature with composition are no longer as great because H_2O can no longer continue to build up in the melt and alkali feldspar begins to evolve along a path similar to an isothermal solvus section. Both of these path segments are very small and would likely lead to a very homogeneous alkali feldspar, as is commonly found in low-temperature granites.

Figure 3b indicates the variations in phase proportions for this composition during H_2O-unbuffered equilibrium crystallization. Importantly, under H_2O-unbuffered conditions, once the magma is saturated with two feldspars, coprecipitation takes place throughout the crystallization interval, and there is a continuous increase in the proportions of each feldspar from the onset of precipitation to the solidus temperature.

The equilibrium crystallization path shown in Figure 3a characterizes the feldspar evolution of wet granitic magmas. This trend should give rise to the normally zoned plagioclase and relatively homogeneous alkali feldspar commonly found in many granitic rocks. These characteristics may be quite different, however, for high-temperature, relatively dry, granitic magmas. The discussion below presents the results of calculations that were designed to assess the differences between such low-temperature paths and those for high-temperature trachytes, syenites, and granites (e.g., fayalite-bearing granites).

Feldspar crystallization in trachytic and syenitic magmas

H_2O-buffered paths in the feldspar system

Crystallization trends for trachytes under H_2O-buffered conditions were discussed in detail in Nekvasil (1990). These trends provide an important basis for comparison with the H_2O-unbuffered paths. For example, Figure 4a shows the evolution of a Sierra el Virulento composition of Moll (1981) modified by removing all of the normative Qz component so that the composition lies within the feldspar system, at 5 kbar at constant H_2O activity, for activity of H_2O, a_{H_2O}, equal to 0.1 (~1.6 wt% H_2O). Un-

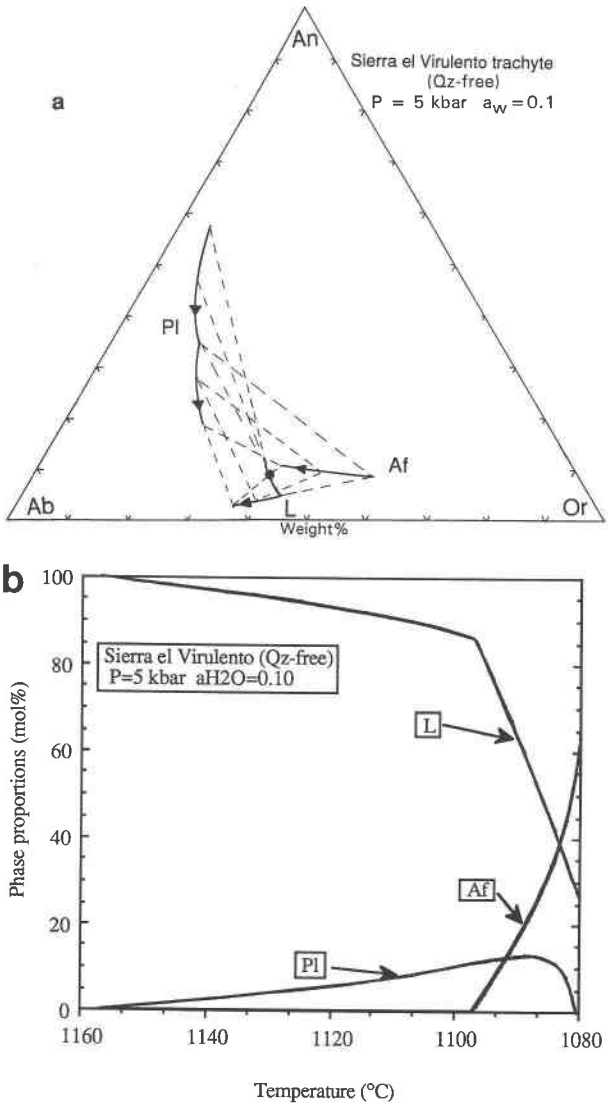

Fig. 4. Portion of the calculated H_2O-buffered equilibrium crystallization path for a model Qz-free Sierra el Virulento trachyte (39.3 wt% Or, 52.0 wt% Ab, 8.67 wt% An) at 5 kbar and activity of H_2O (a_{H_2O}) equal to 0.1. (**a**) Melt (L), plagioclase (Pl), and alkali feldspar (Af) compositions projected into the feldspar system. Arrowheads point to the direction of decreasing temperature. Once all of the plagioclase is resorbed, ternary alkali feldspar precipitates alone, and its composition follows a slightly curved path, not shown, toward the bulk composition. At the onset of alkali feldspar precipitation, there is a slight curvature of the liquid path toward Or (which is difficult to discern in the diagram) that results in coprecipitational behavior during the early stages of precipitation of two feldspars. (**b**) Variations in proportions (mol%) of melt (L), plagioclase (Pl), alkali feldspar (Af), and quartz (Qz) vs. temperature during equilibrium crystallization shown until the plagioclase is completely resorbed. Plagioclase resorption takes place when its curve has a negative slope. All phase proportions sum to $(1 - X_{H_2O}) \times 100$.

der H_2O-buffered conditions, the crystallization temperature interval is small, and the feldspars follow a path similar to an isothermal solvus section. Before the solidus temperature is reached, however, all of the plagioclase is resorbed, and the feldspar path leaves the solvus.

Figure 4b shows the variations in phase proportions during H_2O-buffered equilibrium crystallization of the Qz-free trachyte at 5 kbar. Plagioclase is the liquidus phase and increases in abundance steadily with falling temperature until alkali feldspar appears. At this point, further precipitation of plagioclase is slowed down until a reaction between melt and plagioclase begins, which results in a decrease in abundance of plagioclase and a concomitant increase in the abundance of alkali feldspar with decreasing temperature. This reaction continues until all of the plagioclase is consumed. Crystallization of a single ternary alkali feldspar begins at this point (not shown in Figs. 4a or 4b) and continues until its composition is that of the bulk rock composition.

The resorption of plagioclase in Figure 4b arises from the termination of the 2 feldspar + L surface within the feldspar system at low H_2O activities and the peritectic-like (odd) nature of this surface as the termination is approached. See Nekvasil (1990) and Nekvasil and Lindsley (1990) for further discussion. As discussed by Nekvasil (1990), crystallization of trachytes need not lead to complete resorption of plagioclase; rather, the extent of resorption of plagioclase will depend on the pressure, the bulk H_2O content, and the bulk composition. Partial to complete resorption of plagioclase can also occur for Qz-normative trachytes and syenites and high-temperature granites under H_2O-buffered conditions, particularly if Qz saturation is not attained until the late stages of crystallization.

The feldspars of many natural trachytes show this type of compositional trend (Fig. 4), e.g., southeast Queensland (Ewart, 1981), Sierra el Virulento (Moll, 1981). However, before conclusions are drawn that these trachytes crystallized under H_2O-buffered conditions, the differences between H_2O-buffered and H_2O-unbuffered paths must be assessed.

H_2O-unbuffered paths in the feldspar system

Equilibrium crystallization paths of the projected Sierra el Virulento composition were calculated for H_2O-unbuffered conditions for several bulk H_2O contents, in order to evaluate the differences between the compositional evolution of the feldspars crystallizing under H_2O-unbuffered conditions vs. H_2O-buffered conditions and to compare such paths with those of granite compositions. Figure 5 shows the calculated equilibrium crystallization path of the Qz-free projected Sierra el Virulento composition at 5 kbar and 25 mol% (2.2 wt%), 20 mol% (1.7 wt%), and 15 mol% (1.2 wt%) bulk H_2O contents. For these calculations, the H_2O content increases continually to saturation, at which stage a separate fluid phase appears, which, for modeling purposes, consists of 100% H_2O.

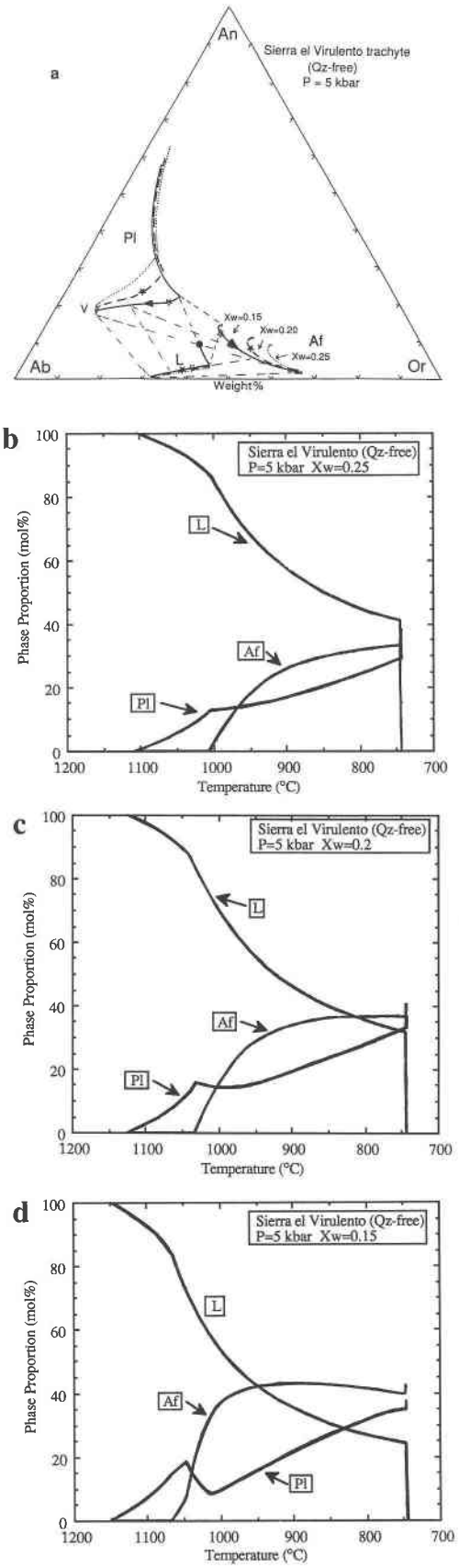

For all of the three bulk H_2O contents, plagioclase is the liquidus phase. Its early compositional evolution, before the magma becomes saturated with a second feldspar, is similar to the H_2O-buffered case and would be difficult to distinguish from it. Once a second feldspar is stabilized, however, the similarities end; plagioclase now no longer changes its composition by following a path similar to an isothermal solvus section, as is generally the case for H_2O-rich magmas or H_2O-buffered magmas, that is, a path dominated by decreasing An content, but instead follows a path dominated by decreasing Or content. Plagioclase follows this path until the liquid becomes saturated in H_2O. From this point on, as the temperature decreases, the H_2O content is buffered by the presence of a fluid, and plagioclase changes its composition along an H_2O-buffered trend similar to that in Figure 3a. However, because of the low bulk H_2O content, H_2O saturation is attained only very close to the solidus temperature, and this path is followed for only a very short distance.

The alkali feldspar compositions also show a very distinctive evolutionary trend. The alkali feldspar compositions describe a loop reflecting the competing effects of increasing Ab content of the melt, which drives the compositions along a path subparallel to an isothermal section in the direction of decreasing Or content, and the effect of the continual temperature depression, which results in a widening of the solvus and hence an increase in the Or content of the alkali feldspar, as shown in Figure 2. For this H_2O-unbuffered Qz-free trachyte composition, the effect of decreasing temperature on expanding the solvus, induced by the increasing H_2O content of the melt, is much stronger than the effect of the change in melt composition. Therefore, the evolving alkali feldspar compositions show a strong enrichment in Or content with

←

Fig. 5. Calculated H_2O-unbuffered equilibrium crystallization path for the model Sierra el Virulento Qz-free trachyte at 5 kbar and bulk H_2O contents of 2.2 wt% (X_{H_2O} = 0.25; dotted curves), 1.7 wt% (X_{H_2O} = 0.20; dashed curves) and 1.2 wt% (X_{H_2O} = 0.15, solid curves). **(a)** Melt (L), plagioclase (Pl), and alkali feldspar (Af) compositions projected into the feldspar system for each bulk H_2O content. Arrowheads point to the direction of decreasing temperature. V indicates the onset of fluid saturation. For all of these curves, resorption begins when the solvus is intersected. Solid stars (X_{H_2O} = 0.20) and open stars (X_{H_2O} = 0.15) indicate the compositions of all phases when partial resorption of plagioclase is replaced by coprecipitation of both feldspars for 20 mol% bulk H_2O content. **(b)** Variations in proportions (mol%) of melt (L), plagioclase (Pl), alkali feldspar (Af) vs. temperature for 2.2 wt% bulk H_2O (X_{H_2O} = 0.25) content. **(c)** Variations in proportions (mol%) of melt (L), plagioclase (Pl), alkali feldspar (Af) vs. temperature for 1.7 wt% bulk H_2O (X_{H_2O} = 0.20) content. The solid star indicates the onset of coprecipitational behavior. **(d)** Variations in proportions (mol%) of melt (L), plagioclase (Pl), alkali feldspar (Af) vs. temperature for 1.2 wt% bulk H_2O (X_{H_2O} = 0.20) content. The open star indicates the onset of coprecipitational behavior. All phase proportions for each bulk H_2O content sum to $(1 - X_{H_2O}) \times 100$.

falling temperature. This enrichment continues until H_2O saturation is reached, at which point the alkali feldspar changes composition once again, as in the buffered case, that is, subparallel to an H_2O-saturated isothermal section.

For lower bulk H_2O contents, the plagioclase composition at the onset of alkali feldspar crystallization is more ternary than for higher bulk H_2O contents (and hence lower temperatures), and the first feldspar pair lies closer to the consolute curve, which connects the consolute points of isothermal sections of the two-feldspar solvus. Since the bulk composition is the same for all the paths in Figure 3a, and the H_2O content in the melt builds up to saturation for all the paths, the final assemblage and the solidus temperature will be the same for all the paths. Therefore, the amount of Or enrichment in the alkali feldspar that will occur during crystallization will increase with decreasing bulk H_2O content. Furthermore, the lower the bulk H_2O content, the smaller the change in An content of the plagioclase during crystallization once alkali feldspar is stable (Fig. 5a). In fact, for $X_{H_2O} = 0.15$, plagioclase compositions evolve almost along an An isopleth.

The changes in phase proportions for the paths in Figure 5a are shown in Figures 5b–5d. As can be seen by comparing Figures 5b and 5c, the extent of decrease in plagioclase abundance during crystallization increases with lower bulk H_2O content. Importantly, unlike the buffered case (Fig. 4b, and Nekvasil, 1990), resorption of plagioclase ceases and coprecipitation commences during the later stages of crystallization. This will not occur for any buffered path, whether or not plagioclase undergoes partial or complete resorption. The temperature of onset of coprecipitational behavior is very similar for $X_{H_2O} = 0.15$ and 0.20 (cf. Figs. 5c and 5d). At the lower bulk H_2O content (Fig. 5d), this temperature is attained at a later stage of evolution than at the higher bulk H_2O content of Figure 5c. This can be readily seen by comparing the fraction of liquid remaining at the onset of coprecipitational behavior for the two bulk H_2O contents (Figs. 5c and 5d). For $X_{H_2O} = 0.25$ (Fig. 5b), this temperature is reached just as both feldspars become stable, and no resorption of plagioclase takes place during crystallization. Until further calculations are conducted with other bulk compositions, it is unclear whether the relatively invariant temperature of the onset of coprecipitation of two feldspars is fortuitous for this bulk composition or a requirement of the system.

At even lower H_2O contents, a significant change in the feldspar crystallization path occurs. As for the other H_2O contents, at 10 mol% (0.75 wt%) bulk H_2O content (Fig. 6), plagioclase is the liquidus phase. As temperature drops and crystallization continues, the composition of the plagioclase becomes more ternary and approaches the solvus. Now, however, the temperatures are higher and the relevant region of the solvus lies farther from the Ab-An sideline. Because of this, the solvus is not intersected at an early stage of crystallization, and the plagioclase compositional path now traverses on the solidus around the nose of (but above) the solvus and toward the alkali feldspar side of the consolute curve. Such a path was also deduced geometrically by W. L. Brown (personal communication, 1990). Once the feldspar composition has passed around the nose of the solvus, crossed the extension of the consolute curve (i.e., the curve connecting the consolute points of the isothermal solvus sections), and entered the alkali feldspar field, the melt compositions begin to evolve along the break in slope that extends past the terminations of the 2 feldspar + L H_2O-isoplethal curves describing the 2 feldspar + L surface. As crystallization continues, the single feldspar evolves along a curved path toward lower An contents around the solvus, as the melt continues to follow this break in slope of the liquidus surface. The melt H_2O content continues to increase and the 2 feldspar + L H_2O-isoactivity curves (and hence, the 2 feldspar + L surface) extend farther and farther toward Ab until they finally catch up with the melt at point A (Fig. 6a), at which point the solvus is intersected by the feldspar path. At this point, an albitic plagioclase begins to crystallize with the earlier formed feldspar, which now has the compositional characteristics of an alkali feldspar. Continued crystallization results in a slight increase in An content with a more major decrease in Or content of the plagioclase, while the alkali feldspar composition undergoes a major increase in Or content. At the very end stages of crystallization, the melt becomes H_2O saturated, and the plagioclase undergoes a slight decrease in An content and the alkali feldspar a slight decrease in Or as the H_2O-saturated polythermal solvus section is followed.

Figure 6b shows the variations in phase proportions during crystallization. This differs dramatically from Figures 5b–5d because of the prolonged crystallization of the first feldspar, which changes in compositional characteristics from plagioclase to alkali feldspar. Additionally, once the second plagioclase feldspar begins to crystallize, the proportions of the first feldspar decrease, that is, alkali feldspar undergoes partial resorption during the later stages of crystallization.

Effect of pressure. The effect of pressure on the H_2O-unbuffered equilibrium crystallization paths is shown in Figure 7a for 15 mol% bulk H_2O content by juxtaposition of the calculated 5-kbar (dashed curves) and 2-kbar (solid curves) crystallization paths. The higher temperatures of the 5-kbar path during the early stages of crystallization result in feldspar compositions that move closer to the consolute curve of the solvus than at 2 kbar. The higher H_2O content at saturation at 5 kbar (and hence lower solidus temperature), however, results in more extensive Or enrichment of the alkali feldspar, Or depletion of plagioclase, and Or depletion of the liquid during the late stages of crystallization. Figure 7b shows the variations in phase proportions at 2 and 5 kbar. Because the 5-kbar feldspar path reaches compositions closer to the consolute curve, and because melt compositions move further into the odd region of the 2 feldspar + L surface during

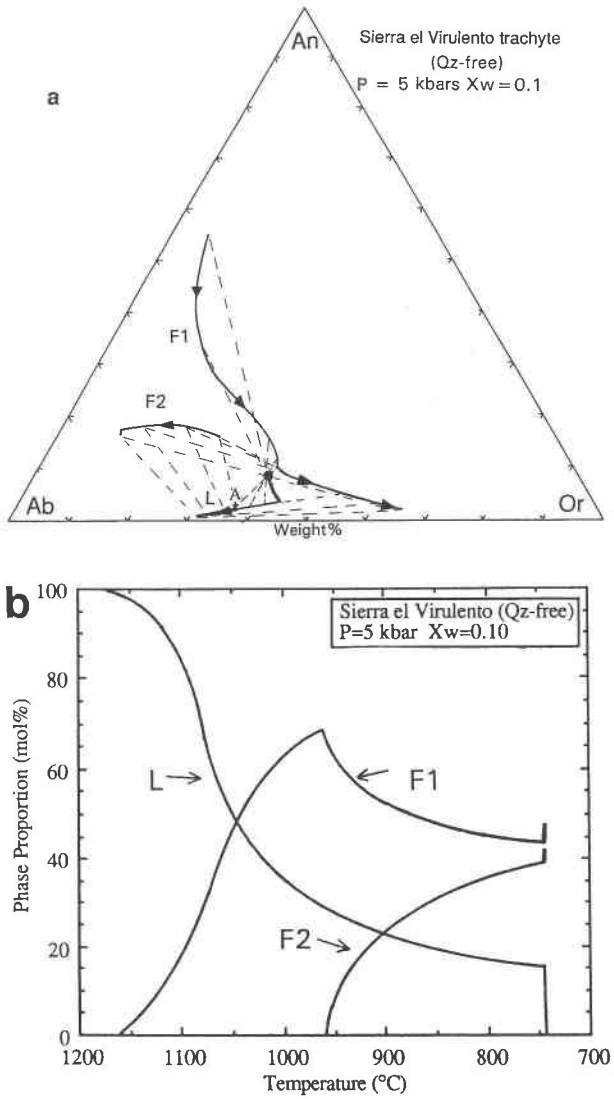

Fig. 6. Calculated H_2O-unbuffered equilibrium crystallization path for the model Qz-free Sierra el Virulento trachyte at 5 kbar and 0.75 wt% ($X_{H_2O} = 0.1$) bulk H_2O content. (**a**) Melt (L), the first feldspar (F1) and the second feldspar (F2) compositions projected into the feldspar system. Arrowheads point to the direction of decreasing temperature. Point A refers to the point on the liquid path where the 2 feldspar + L surface reaches the melt composition and two feldspars are stabilized. (**b**) Variations in proportions (mol%) of melt (L), first feldspar (F1), and second feldspar (F2) vs. temperature during equilibrium crystallization. All phase proportions sum to $(1 - X_{H_2O}) \times 100$.

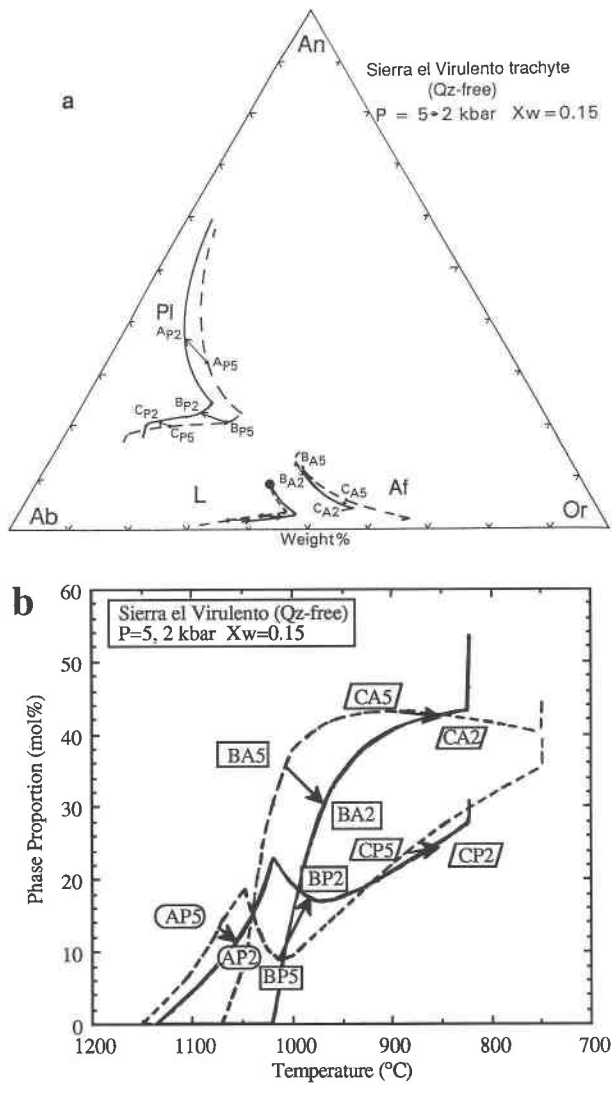

Fig. 7. Calculated H_2O-unbuffered equilibrium crystallization path for the model Sierra el Virulento Qz-free trachyte at 5 kbar and 2 kbar and 1.2 wt% ($X_{H_2O} = 0.15$) bulk H_2O content. (**a**) Melt (L), plagioclase (Pl), and alkali feldspar (Af) compositions at 5 kbar (dashed curves) and 2 kbar (solid curves) projected into the feldspar system. Arrows indicate three decompressional stages: Path A, where only plagioclase and melt are present and decompression commences at 1125 °C with a gradient of 7 °C/kbar. The plagioclase composition changes from A_{P5} to A_{P2}. In path B, plagioclase, alkali feldspar, and melt are present at higher pressure, and decompression commences at 1020 °C. The plagioclase composition changes from B_{P5} to B_{P2}; the alkali feldspar composition changes from B_{A5} to B_{A2}. In path C, plagioclase, alkali feldspar, and melt are present at higher pressure, and decompression commences at 880 °C. The plagioclase composition changes from C_{P5} to C_{P2}; the alkali feldspar composition changes from C_{A5} to C_{A2}. (**b**) Variations in proportions of plagioclase and alkali feldspar (mol%) at 5 kbar (dashed curves) and 2 kbar (solid curves) with arrows indicating decompressional pathways as described in **a**.

the early stages of crystallization, more resorption of plagioclase takes place during crystallization at higher pressures.

The effect of decompression can also be seen in Figure 7. It is much more complex for trachytic and syenitic magmas than for wetter granitic magmas (see Nekvasil, 1991), and the behavior exhibited depends greatly upon the stage of crystallization (that is, the assemblage) just

prior to ascent. As a first case, if decompression occurs when plagioclase is the only crystalline phase present at 5 kbar (path A in Fig. 7), and decompression follows an average gradient of 7 °C/kbar (Sykes and Holloway, 1987), then the system must readjust itself in order to reestablish equilibrium by undergoing some melting of the higher pressure plagioclase. This can be seen in the phase proportion diagram of Figure 7b by the slightly negative slope of the arrow A_{P5} to A_{P2}. The effects on plagioclase composition are indicated in Figure 7a, and they show that the lower pressure plagioclase would be more anorthitic than the previously formed higher pressure plagioclase. Texturally, this may be indicated by an irregular boundary around cores of plagioclase (induced by partial melting), mantled by a zone of more anorthitic plagioclase (reverse zone), followed by normal zoning (if a stepwise fractional crystallization process takes place).

If decompression does not begin until alkali feldspar has appeared, and plagioclase is undergoing reaction with a liquid (path B in Fig. 7), then plagioclase will precipitate upon decompression, as shown by the positive slope of the phase proportion arrow B_{P5} to B_{P2} in Figure 7b. The higher pressure alkali feldspar on the other hand will undergo a significant amount of melting, as its lower pressure equilibrium abundance is about 35% lower than at 5 kbar (as shown by the arrow B_{A5} to B_{A2}). The plagioclase will become slightly more anorthitic (but not show as much An enrichment as for path A), but Or poor. The alkali feldspar may become reversely zoned with a slight increase in Or and decrease in An content at the lower pressure. As the result of decompression, the melt will become enriched in Or.

Path C indicates the effects of decompression on the high-pressure assemblage if decompression occurs once plagioclase and alkali feldspar are coprecipitating (toward the later stages of crystallization). In this case, it is possible to get essentially no change in the abundances of the phases and to affect only their compositions. For example, for path C in Figure 7b, the arrows (C_{P5} to C_{P2} for plagioclase and C_{A5} to C_{A2} for alkali feldspar) show a nearly zero slope. However, as shown in Figure 7a, the slight An enrichment and Or depletion of plagioclase and the Or enrichment of the melt, as was seen for path B, are still manifested, but the magnitude of the enrichment of each component declines. The change in composition be-

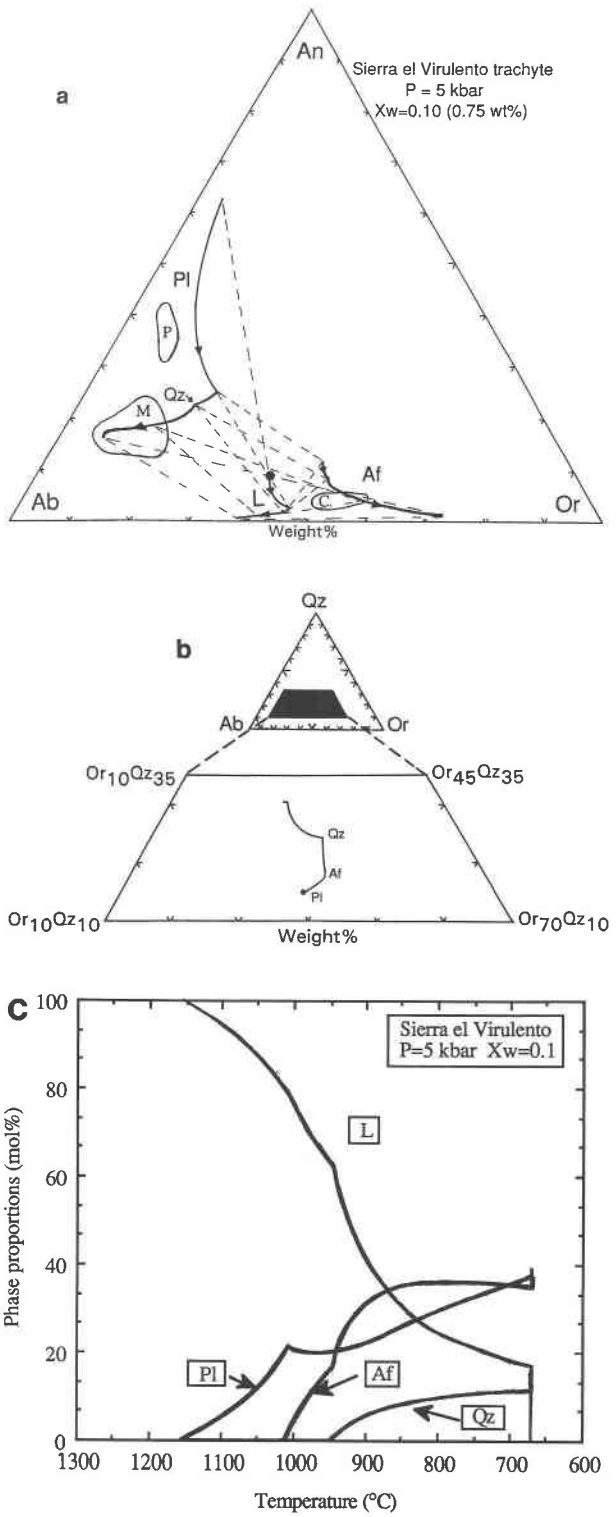

←

Fig. 8. Calculated H_2O-unbuffered equilibrium crystallization path for the Sierra el Virulento trachyte (33.9 wt% Or, 44.7 wt% Ab, 7.45 wt% An, 14.0 wt% Qz) at 5 kbar and 0.75 wt% (X_{H_2O} = 0.10) bulk H_2O content. (**a**) Melt (L), plagioclase (Pl), and alkali feldspar (Af) compositions projected into the feldspar system. The symbol Qz indicates the onset of crystallization of quartz. Arrowheads point to the direction of decreasing temperature. The three outlined regions refer to the plagioclase (P), mesoperthite (M), and cryptoperthite (C) of Parsons and Brown (1988). (**b**) Melt compositions projected into the system Ab-Or-Qz. Each inflection marks the onset of precipitation of a new crystalline phase, plagioclase (Pl), alkali feldspar (Af), and quartz (Qz). The last inflection marks the beginning of stability of a fluid phase. (**c**) Variations in proportions (mol%) of melt (L), plagioclase (Pl), alkali feldspar (Af), and quartz (Qz) vs. temperature during equilibrium crystallization.

comes smaller and smaller as decompression brings the temperature closer and closer to the low-pressure solidus temperature. The change in alkali feldspar composition upon decompression is more pronounced than in path B. Instead of the Or enrichment shown in path B, there will be a slight Ab enrichment. Just as for plagioclase, this trend will be enhanced closer to the low-pressure solidus temperature.

H_2O-unbuffered paths of Qz-normative trachytes and syenites

Natural trachytes differ from compositions within the feldspar system by containing ferromagnesian components, and they are commonly quartz or nepheline normative. The Sierra el Virulento trachyte studied here is quartz normative, and the effect of a buildup of the Qz component in the liquid was investigated computationally for this composition to determine the differences between crystallization paths that are closer to natural compositions and those within the feldspar system.

Figure 8a shows the projected path of the Qz-normative Sierra el Virulento composition in the feldspar system for 10 mol% bulk H_2O content at 5 kbar. The effect of dilution of the feldspar components by the Qz component can be readily seen by comparing Figure 8a with Figures 5a and 6a. The crystallization path for the Qz-normative composition at 10 mol% H_2O is similar to that for higher H_2O contents because of the temperature depression induced by dilution. Beyond the temperature differences, the only differences between this path and paths in the feldspar system are the inflections in the feldspar and liquid paths caused by the precipitation of quartz, which diminishes the continual dilution of the feldspar components (which had been occurring before Qz saturation through the buildup of a Qz component and H_2O in the melt and through precipitation of the feldspars themselves). Figure 8b shows the melt path projected into the haplogranite system showing the inflections in the melt evolutionary path more clearly.

Figure 8c shows the variations in phase proportions during crystallization of this composition. The odd region of the 2 feldspar + L surface in the granite system is intersected by the melt path, and hence partial resorption of plagioclase does occur for this composition. Importantly, however, the even (cotecticlike) portion of the 2 feldspar + Qz + L surface is reached upon saturation with quartz, and coprecipitation of feldspars occurs once quartz appears. The amount of resorption that will occur is very dependent upon the bulk H_2O content. With sufficiently low bulk H_2O contents (<0.2 wt%), it may be possible for the melt to intersect the very small odd region of the 2 feldspar + Qz + L surface. At this point it must again be pointed out that the predicted highest bulk H_2O content for which an H_2O-buffered path will enter the odd region of the 2 feldspar + Qz + L surface at some stage of the crystallization interval depends upon the ternary solid solution model chosen. The model of Lindsley and Nekvasil (1989) overestimates the amount of ternary solution in both feldspars at a given pressure, while the model of Nekvasil and Burnham (1987) quite likely underestimates the amount of ternary solution. Use of the former model, therefore, results in an overestimation of the highest bulk H_2O content (for which a crystallization path of a trachytic magma would enter the odd portion of the 2 feldspar + Qz + L surface), whereas the latter model probably underestimates this value.

H_2O-unbuffered paths of high-temperature granites

Figure 9a shows the evolution of feldspars and melt during equilibrium crystallization for the same model rhyolite as in Figure 3 but under conditions of low bulk H_2O content. The crystallization path is very similar to that for the Qz-free composition at a higher bulk H_2O content. Importantly, the evolutionary path of the feldspars is very similar to that for the trachyte, in that, upon stabilization of two feldspars, plagioclase compositions change mainly by decreasing Or content, whereas alkali feldspar changes mainly by increasing Or content. This path is very different from that for wet, low-temperature granites (cf. Figs. 9a and 3a). However, this difference is only manifested for H_2O-unbuffered conditions. For H_2O-buffered conditions, both the wet and dry model rhyolite show the same general path as seen in Figure 4a, with the main difference being in the extent of ternary solution. In fact, the wet H_2O-unbuffered path does not even differ very much from the H_2O-buffered path.

When Figure 9a is compared with Figure 8a, it is readily apparent that toward the end stages of H_2O-unbuffered crystallization of a trachyte, the feldspar and melt compositions are very similar to those of a granite or rhyolite. This implies that from the standpoint of the behavior of the feldspars, it is possible to derive low-temperature, wet granitic melts from trachytic magmas simply by H_2O-unbuffered crystallization. Trachytes crystallizing under H_2O-buffered conditions could readily produce high-temperature granites during late stage crystallization.

Implications for natural syenites, trachytes, and high-temperature granites

A natural magma may undergo various stages of H_2O evolution. During the early high-temperature stage, in which perhaps fayalitic olivine and pyroxenes precipitate, the H_2O content would build up continuously, and crystallization would proceed under H_2O-unbuffered conditions. However, once hydrous minerals (e.g., biotite) became stable, the buildup of H_2O in the melt (because of crystallization of anhydrous phases such as feldspars) would result in the production of more biotite. As long as the melt contains sufficient ferromagnesian components to continue producing biotite, the magma would crystallize under H_2O-buffered conditions. This should continue until the abundance of the ferromagnesian components in the melt becomes too small to permit a sufficient increase in the abundance of biotite to buffer the H_2O content. From this stage on, the H_2O content of the

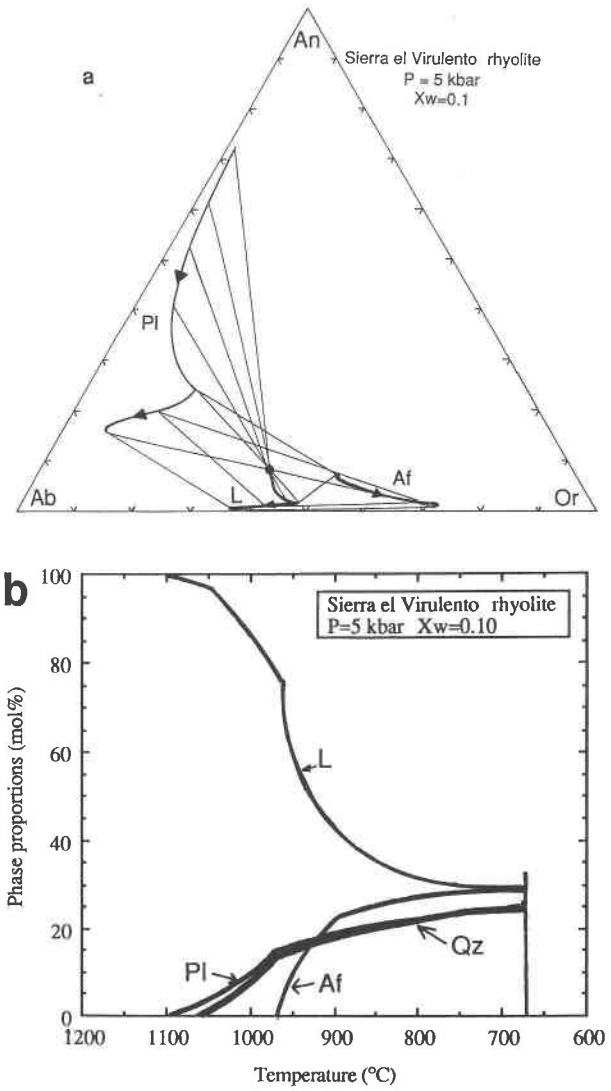

Fig. 9. Calculated H_2O-unbuffered equilibrium crystallization path for the model Sierra el Virulento rhyolite (28.5 wt% Or, 37.5 wt% Ab, 5.88 wt% An, 30.0 wt% Qz) at 5 kbar and 0.75 wt% ($X_{H_2O} = 0.10$) bulk H_2O content. (**a**) Melt (L), plagioclase (Pl), and alkali feldspar (Af) compositions projected into the feldspar system. Quartz appears soon after plagioclase, so the inflections in the feldspar paths seen in Figure 7a do not occur. Arrowheads point to the direction of decreasing temperature. (**b**) Variations in proportions (mol%) of melt (L), plagioclase (Pl), alkali feldspar (Af), and quartz (Qz) vs. temperature during equilibrium crystallization. All phase proportions sum to $(1 - X_{H_2O}) \times 100$.

melt would once again increase and build up to saturation with an aqueous fluid. Under such conditions, however, the same basic trends would be seen as for the H_2O-unbuffered conditions, with, however, a chance of more ternary feldspar compositions and the possibility of more resorptional behavior as well as greater Or depletion of plagioclase and Or enrichment of alkali feldspar during the late stages of crystallization.

The effect of additional melt components and mineral phases must be considered when applying the above paths to the interpretation of natural rocks. The ferromagnesian melt components and the crystalline phases olivine, pyroxene, and biotite are predominantly those of interest. The olivine and pyroxene melt components will have a definite effect on plagioclase composition. The anorthite content of plagioclase is very sensitive to the activity of the An melt component. This sensitivity to even slight variations in anorthite activity, when coupled with the decrease in An activity because of the strong negative deviations from ideality characterizing the mixing behavior of the anorthite and olivine (and to a lesser extent pyroxene) melt components, results in a significant decrease in the An content of the plagioclase. These deviations from ideality are exemplified in the system An-Fo (Andersen, 1915; Osborn and Tait, 1952), where negative deviations from ideality are so strong as to result in compound formation, as evidenced by the crystallization of spinel. The effect of ignoring the ferromagnesian components can be seen from the work of Housch and Luhr (1991). They compared calculated plagioclase compositions using the Nekvasil (1986) and Burnham and Nekvasil (1986) models with experimentally grown plagioclase presumed in equilibium with late stage melts from basaltic magmas. As could be expected from the strong negative deviations from ideality of the An melt component with ferromagnesian melt components, even small amounts of these latter components in the melt resulted in calculated An contents in plagioclase that are too high. This is not a major problem for this analysis because only the trends are discussed. Additionally, the uncertainty of location of any compositional point in P-T space induced by ignoring the ferromagnesian components is outweighed by the differences induced by using various solid solution models.

In addition to the effect of buffering the H_2O activity of the melt, precipitation of biotite may have a significant effect on the crystallization paths of the feldspars because biotite preferentially incorporates Or component relative to the other feldspar components and changes the evolutionary path of the melt. It is difficult to predict the magnitude of the effect of biotite because it depends on the stage of feldspar evolution at which biotite first appears. The stability relations of high-temperature (e.g., Ti-rich) biotite are only poorly known, and much experimental work remains to be done before the importance of biotite in dictating the evolutionary paths of the feldspars can be evaluated.

Because of the marked differences between the feldspar compositional trends of H_2O-buffered and H_2O-unbuffered trachytes, it should be possible to use natural feldspar zoning patterns to get an indication of the behavior of H_2O during crystallization of the magma. However, ternary feldspars in natural syenites commonly have undergone considerable subsolidus exsolution (e.g., Fuhr-

man et al., 1988), which has modified any previously existing zonation. In rare cases, however, it is possible to glean some information on the nature of zoning within ternary feldspars. Careful work by Parsons and Brown (1988), for example, on the perthitic feldspars of the Klokken intrusion in South Greenland has yielded important information regarding feldspar zoning in syenites. Their syenodiorite KB50 and syenite KB56 show three clusters of feldspar compositions (shown in Fig. 8) that seem to agree with the compositional types of feldspars produced by crystallization under H_2O-unbuffered conditions. These clusters are, in contrast, quite different from those that might be expected for crystallization under H_2O-buffered conditions (exemplified in Fig. 4a). Although the feldspar zoning pattern is not truly definitive, Parsons and Brown's (1988) analyses of zoned ternary feldspars of the Klokken intrusion show plagiocase zoned in the usual manner, that is, by decreasing An content, sodic sanidine (their cryptoperthite) zoned by increasing Or content, and ternary oligoclase (their "mesoperthite") in which there is some evidence of zoning by decreasing Or content.

In volcanic rocks, rapid cooling makes late stage zonation and the compositions of groundmass phases more difficult to obtain. Efforts by Ferguson (1978) to evaluate the compositions of zoned feldspars in trachytic lavas from central Victoria indicate that most of the feldspars from the Turritable Falls trachyte flow are zoned such that the feldspar compositions move subparallel to an isothermal solvus section as if the magma were buffered with respect to H_2O content. However, he notes the presence of pegmatoidal clots and veins in which the alkali feldspar shows reverse zoning (in some cases from Or_{48} to Or_{60}). This could be a natural example of a path that involves early buffering of the H_2O content and later buildup of H_2O during crystallization.

Natural examples of crystallization of a single feldspar around the nose of the solvus are understandably rare because of the very low H_2O activities required. A natural example may be found in the Mboutou layered gabbro-syenite-granite complex of northern Cameroon. Parsons et al. (1986) report feldspars forming a compositional continuum with a compositional range from $An_{85}Or_2$ to $Or_{55}An_1$ in the Mboutou. The rock types within the complex, however, are quite diverse, and comparison of the feldspars among these rock types requires that they be related through a differentiation process.

Reverse zoning of alkali feldspar in Qz-normative trachytes, pantellerites, comendites, and phonolites have been widely reported, e.g., Carmichael (1965), Nash et al. (1969), Nicholls and Carmichael (1969), and the origin of such zoning has remained a source of debate. Because many of these rock types show peralkaline characteristics, it was natural for early workers to link this zoning behavior to peralkalinity through the postulation of complex fractionation curves for feldspars in alkali-rich magmas (e.g., Nash et al., 1969). The results of the calculations summarized above indicate that reversely zoned alkali feldspar may result from as simple a process as stepwise equilibrium crystallization of a dry felsic magma and does not require excess alkalis. Such H_2O-unbuffered behavior may also explain the reverse zones in alkali feldspars from rocks such as pantellerites, in which only a single feldspar crystallizes (alkali feldspar) because the Or enrichment can be readily linked to the expansion of the An-free alkali feldspar solvus.

From the above analysis of feldspar crystallization behavior, it is reasonable to conclude that differentiation of high-temperature syenitic magmas can produce magmas with the compositional characteristics of wet granitic melts, as long as the syenitic magma crystallizes under H_2O-unbuffered conditions (at least during the late stages of its evolution). In contrast, high-temperature syenitic magmas crystallizing under H_2O-buffered conditions can only give rise to high-temperature granitic magmas. For any particular association of syenites and granites, however, a fractionation relationship between the two rock types can be accepted only after detailed isotopic and trace element analysis.

The above discussion centered on an investigation of equilibrium crystallization pathways. Natural crystallization processes are probably a combination of equilibrium and fractional crystallization paths. For high-temperature felsic magmas, ideal fractional crystallization paths can differ significantly from equilibrium crystallization paths. Melts reaching the 2 feldspar + L surface on its even side during fractional crystallization will evolve along the surface, precipitating two feldspars as the bulk composition changes and the H_2O content increases. Once the neutral curve is reached, only a single feldspar becomes stable, and the melt moves off of the surface and onto the ternary alkali feldspar liquidus surface. With continual buildup of H_2O, however, the melt will quite likely reach the surface again because of the shift of the surface toward lower An contents and its extension toward Ab with increasing H_2O content. The details of stepwise fractional crystallization and of equilibrium melting and stepwise fractional melting paths will be the subjects of future articles.

The calculated paths discussed above serve to indicate the importance of feldspar zoning in providing important information regarding conditions and processes relevant to the crystallization of felsic magmas. They further illustrate that before we can evaluate the effects of open system and kinetic processes at work in magmatic systems, we must further our understanding of the equilibrium state toward which systems strive. Particularly among felsic rocks, where bulk compositions are so similar and the mineral relations fairly indistinct, feldspar zoning may provide an important key to unraveling the evolutionary history of a magma.

Acknowledgments

The careful reviews of S.A. Morse and J.S. Beard contributed greatly to this manuscript. Support for computational services from the Department of Earth and Space Sciences, SUNY–Stony Brook, and partial sup-

port from NSF grant EAR-8916050 and the Center for High Pressure Research are gratefully acknowledged.

References cited

Abbott, R.N., Jr. (1978) Peritectic relations in the system An-Ab-Or-Qz-H_2O. Canadian Mineralogist, 16, 245–256.

Andersen, O. (1915) The system anorthite-forsterite-silica. American Journal of Science, 39, 407–454.

Burnham, C.W., and Nekvasil, H. (1986) Equilibrium properties of granite pegmatite magmas. American Mineralogist, 71, 239–263.

Carmichael, I.S.E. (1963) The crystallization of feldspar in volcanic acid liquids. Quarterly Journal of the Royal Society of London, 119, 95–131.

——— (1965) Trachytes and their phenocrysts. Mineralogical Magazine, 34, 107–125.

Ewart, A. (1981) The mineralogy and chemistry of the anorogenic Tertiary volcanics of S.E. Queensland and N.E. New South Wales. Journal of Geophysical Research, 86, B11, 10242–10256.

Ferguson, A.K. (1978) A mineralogical investigation of some trachyte lavas and associated pegmatoids from Camel's Hump and Turritable Falls, central Victoria. Journal of the Geological Society of Australia, 25, 185–197.

Fuhrman, M., Frost, R., and Lindsley, D.H. (1988) Crystallization conditions of the Sybille Monzosyenite, Laramie Anorthosite Complex, Wyoming. Journal of Petrology, 29, 699–729.

Housch, T.B., and Luhr, J.F. (1991) Plagioclase-melt equilibria in hydrous systems. American Mineralogist, 76, 477–492.

Johannes, W. (1978) The melting of plagioclase in the system Ab-An-H_2O and Qz-Ab-An-H_2O at P_{H_2O} = 5 kbar, an equilibrium problem. Contributions to Mineralogy and Petrology, 66, 295–303.

Lindsley, D.H., and Nekvasil, H. (1989) A ternary feldspar model for all reasons. Eos, 70, 506.

Moll, E.J. (1981) Geochemistry and petrology of mid-Tertiary ash flow tuffs from the Sierra el Virulento area, eastern Chihuahua, Mexico. Journal of Geophysical Research, 86, B11, 10321–10334.

Nash, W.P., Carmichael, I.S.E., and Johnson, R.W. (1969) The mineralogy and petrology of Mount Suswa, Kenya. Journal of Petrology, 10, 409–439.

Nekvasil, H. (1986) A theoretical thermodynamic investigation of the system Ab-An-Or-Qz(-H_2O) with implications for melt speciation, 268 p. Ph.D. thesis, The Pennsylvania State University, University Park, Pennsylvania.

——— (1988a) Calculation of equilibrium crystallization paths of compositionally simple hydrous felsic melts. American Mineralogist, 73, 956–965.

——— (1988b) Calculated effect of anorthite component on the crystallization paths of H_2O-undersaturated haplogranitic melts. American Mineralogist, 73, 966–982.

——— (1990) Reaction relations in the granite system: Implications for trachytic and syenitic magmas. American Mineralogist, 75, 560–571.

——— (1991) Ascent of felsic magmas and formation of rapakivi. American Mineralogist, 76, 1279–1290.

Nekvasil, H., and Burnham, C.W. (1987) The calculated individual effects of pressure and water content on phase equilibria in the granite system. Geochemical Society Special Publication, 1, 433–445.

Nekvasil, H., and Lindsley, D.H. (1990) Termination of the 2 feldspar + liquid curve in the system Ab-Or-An-H_2O at low H_2O contents. American Mineralogist, 75, 1071–1079.

Nicholls, J., and Carmichael, I.S.E. (1969) Peralkaline liquids: A petrological study. Contributions to Mineralogy and Petrology, 20, 268–294.

Novak, S.W., and Mahood, G.A. (1986) Rise and fall of a basalt-trachyte-rhyolite magma system at Kane Springs Wash caldera, Nevada. Contributions to Mineralogy and Petrology, 94, 352–373.

Osborn, E.F., and Tait, D.B. (1952) The system diopside-forsterite-anorthite. American Journal of Science, Bowen Volume, 413–433.

Parsons, I., and Brown, W.L. (1988) Sidewall crystallization in the Klokken intrusion: Zoned ternary feldspars and coexisting minerals. Contributions to Mineralogy and Petrology, 98, 431–443.

Parsons, I., Brown, W.L., and Jacquemin, H. (1986) Mineral chemistry and crystallization conditions of the Mboutou layered gabbro-syenite-granite complex, North Cameroon. Journal of Petrology, 27, 1305–1329.

Sykes, M.L., and Holloway, J.R. (1987) Evolution of granitic magma during ascent: A phase equilibrium model. Geochemical Society Special Publication, 1, 447–461.

Tuttle, O.F., and Bowen, N.L. (1958) Origin of granite in light of experimental studies in the system $NaAlSi_3O_8$-$KAlSi_3O_8$-SiO_2-H_2O. Geological Society of America Memoir, 74, 153 p.

Manuscript received July 19, 1991
Manuscript accepted January 9, 1992